

Itinerant Antiferromagnetism in FeGe_2

T.E. Mason, C.P. Adams, S.A.M. Mentink, E. Fawcett

Department of Physics, University of Toronto, Toronto, ON M5S 1A7, Canada

A.Z. Menshikov

Institute for Metal Physics, Ekaterinburg, Russia

C.D. Frost, J.B. Forsyth, T.G. Perring

*ISIS Facility, Rutherford Appleton Laboratory, Chilton, Didcot, OX11 0QX,
United Kingdom*

T.M. Holden

AECL, Chalk River Laboratories, Chalk River, ON K0J 1J0, Canada

Abstract

FeGe_2 , and lightly doped compounds based on it, have a Fermi surface driven instability which drive them into an incommensurate spin density wave state. Studies of the temperature and magnetic field dependence of the resistivity have been used to determine the magnetic phase diagram of the pure material which displays an incommensurate phase at high temperatures and a commensurate structure below 263 K in zero field. Application of a magnetic field in the tetragonal basal plane decreases the range of temperatures over which the incommensurate phase is stable. We have used inelastic neutron scattering to measure the spin dynamics of FeGe_2 . Despite the relatively isotropic transport the magnetic dynamics is quasi-one dimensional in nature. Measurements carried out on HET at ISIS have been used to map out the spin wave dispersion along the c-axis up the 400 meV, more than an order of magnitude higher than the zone boundary magnon for wavevectors in the basal plane.

Studies of the spin dynamics of the high T_c superconductor, $\text{La}_{2-x}\text{Sr}_x\text{CuO}_4$, have shown that this material has incommensurate magnetic fluctuations characteristic of a metal close to a spin density wave instability[1]. This has led to a renewed interest in systems which exhibit similar instabilities since there are many unanswered questions regarding the transport and magnetic properties of spin density wave systems. The prototypical SDW system is the itinerant antiferromagnet Cr and dilute alloys of Cr with other transition metals[2]. SDW ordering also occurs in Mott-Hubbard systems where strong correlations lead to a break down of conventional band theory and, as in the high T_c cuprates, a metal insulator transition[3]. FeGe_2 and lightly doped compounds based on it have a similar (Fermi surface) spin density wave instability which drives the system to order and, in its undoped form, exhibits both commensurate and incommensurate magnetic ordering as temperature is varied. We are studying the transport and spin dynamics of this system in order to obtain a better microscopic understanding of how this instability is manifested in the spin fluctuations.

The properties of FeGe_2 , a tetragonal material with the CuAl_2 structure, have been studied since 1943[4] and many of the details of the crystal and magnetic structure have been determined [5–8]. FeGe_2 is characterised by two magnetic phase transitions, the first of which is the Néel transition from a paramagnetic phase to an incommensurate spin density wave state at $T_N = 289$ K in zero field. The second one is a commensurate-incommensurate (C-IC) transition into a collinear antiferromagnetic structure. This transition occurs at $T_c = 263$ K in zero field. The propagation vector \vec{Q} of the SDW is parallel to $[100]$ and varies from 1 to roughly $1.05 a^*$ between the two transitions which are seen in resistivity[9,10], ultrasonic attenuation[11], heat capacity[5,12], and AC susceptibility[13] studies. The spins lie in the basal plane and are ferromagnetically aligned along the c-axis. Although this compound has been well characterised in zero field there has been very little work done in magnetic fields and not much is known about the details of the magnetic phase diagram. The magnon and phonon dispersion were measured (primarily at low temperatures) and revealed a significant anisotropy of the magnetic interactions with the spin wave velocity along the c-axis much higher than that observed for modes propagating in the basal plane [14]. For those thermal neutron triple-axis measurements it was not possible to fully characterise the spin wave dispersion along c due to the unsuitability of that technique for energy transfers beyond about 50 meV.

Incommensurate ordering of the type seen in FeGe_2 gives rise to four magnetic satellites around (100) and related positions occurring at $(1 \pm q, 0, 0)$ and $(1, \pm q, 0)$. Elastic neutron scattering can be used to determine the wavevector of this magnetic ordering, a scan through the incommensurate peaks at 275 K is shown in the upper panel of Figure 1 compared to that of $\text{Fe}(\text{Ge}_{0.96}\text{Ga}_{0.04})_2$ at the same temperature. Doping has the effect of increasing the magnitude

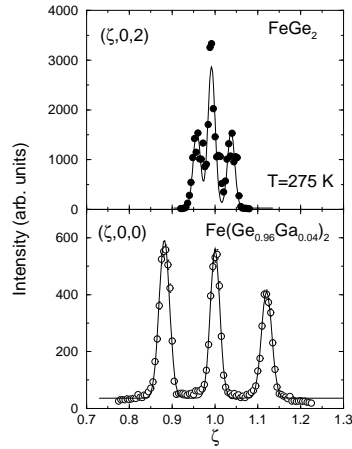


Fig. 1. Scans through the incommensurate magnetic Bragg peaks for pure (upper panel) and Ga doped (lower panel) FeGe_2 at 275 K obtained on the E3 and C5 triple axis spectrometers at Chalk River. The peak in the centre arises from the two peaks displaced from the commensurate position along the b-axis, seen due to the coarse vertical collimation employed in these measurements.

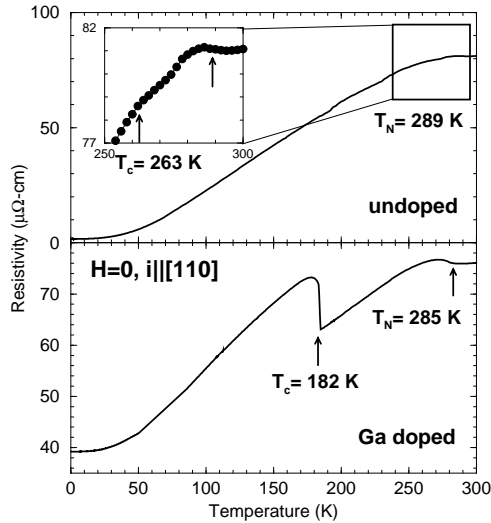


Fig. 2. Temperature dependence of the resistivity for pure and Ga doped FeGe_2 (measured on pieces of the same samples used for Figure 1).

of the incommensurate wavevector (similar to what is seen in lightly doped alloys of $\text{Cr}[2]$). In the 4 at% Ga doped sample the ordering wavevector varies between $q = 0.12$ just below $T_N = 285\text{K}$ and $q = 0.1$ below a first order lock-in transition at $T_c = 182\text{K}$. In the pure material the transition to the low temperature commensurate state (with $\mathbf{q} = 0$) is continuous. The zero field resistivity for these two compounds is shown in Figure 2. In the doped sample (bottom panel) the two phase transitions are clearly visible and are denoted by arrows. In the pure material the anomalies are more subtle but the transitions

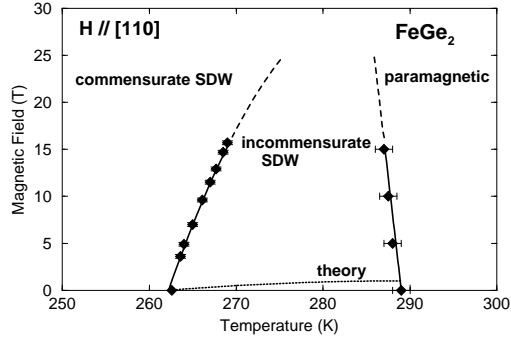


Fig. 3. Magnetic phase diagram for FeGe_2 for a magnetic field applied along the $[110]$ direction determined by resistivity measurements and (for $H=0$) neutron diffraction. The line denoted theory corresponds to the approximate phase boundary expected based on the Ginzburg-Landau theory of Reference [13]

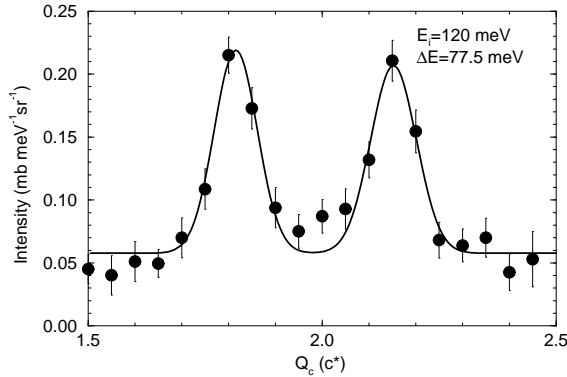


Fig. 4. Constant energy cut at 77.5 meV through the two counter-propagating spin wave modes obtained on HET for FeGe_2 at 11 K using an incident neutron energy of 120 meV.

are seen in the inset. The transition temperatures deduced from the resistive anomalies agree well with those determined by neutron scattering. We have used similar measurements, together with constant temperature, field scans which clearly show the lower phase transition, with a magnetic field applied in the basal plane to determine the magnetic phase diagram for FeGe_2 , shown in Figure 3, the behaviour is similar for a field applied along $[100]$. [15]

In order to fully characterise the ground state of FeGe_2 we have measured the spin dynamics at low temperatures (11 K) using the direct geometry time-of-flight spectrometer HET at ISIS. This instrument allows access to much higher incident neutron energies than the thermal triple-axis measurements of Holden et. al. [14] making it possible to fully map out the c -axis dispersion. Figure 4 shows a constant energy cut through the time-of-flight trajectories of the 2.5 m detector bank on HET for an energy transfer of 77.5 meV. This was obtained for an integrated current of 2200 μA -hrs using an incident energy of 120 meV. The two spin wave modes emanating from $Q_c = 2$ are clearly visible,

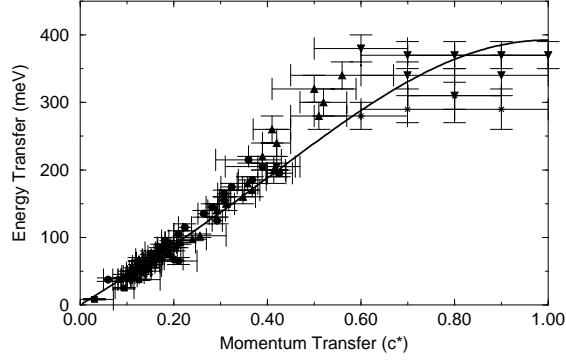


Fig. 5. Spin wave dispersion relation obtained from the triple axis data (lowest energies) and incident energies of 80, 120, 300, 500, and 700 meV on HET. The line is a fit to a model for a planar one-dimensional ferromagnet with a zone boundary magnon energy of 400 meV.

for energies higher than 25 meV FeGe₂ behaves as a quasi-one-dimensional ferromagnet so it is permissible to ignore the variation of Q_a with energy transfer, a fact confirmed by more detailed analysis of these results[16]. By carrying out measurements with incident energies of 80, 120, 300, 500, and 700 meV we have fully mapped out the c -axis dispersion relation which is shown in Figure 5. The line is the result of a fit to a planar one-dimensional ferromagnet model in appropriate in the zero temperature classical limit. The zone boundary magnon energy is 400 meV, more an order of magnitude larger than the 25 meV found for the a -axis[14]. This substantial anisotropy reflects the structure of FeGe₂, the Fe-Fe distance in the c -axis chains of Fe spins is similar to that in pure Fe, whereas in the ab -plane the distance between the Fe ions is 4.2 Å. Along the c -axis the interaction is ferromagnetic and mainly due to d -orbital overlap while in the basal plane the weaker antiferromagnetic coupling has its origins in the conduction electrons.

FeGe₂ is a unique example of quasi-one-dimensional ferromagnetism in an itinerant electron system. Studies of the magnetic dynamics at higher temperatures[16] reveal the presence of well resolved magnon-like excitations even in the paramagnetic state. The much weaker basal plane coupling drives the three dimensional ordering, the doping dependence of the ordering wavevector suggests that this is Fermi surface driven, hole doping by substituting Ga for Ge increases the incommensurate wavevector similar to the effect of increased Sr doping in La_{2-x}Sr_xCuO₄ [1] or V doping in Cr_xV_{1-x}[2]. which are quasi-two-dimensional and three-dimensional realizations of systems which exhibit Fermi surface driven spin density wave instability. The Fe(Ge_{1-x}Ga_x)₂ alloy system represents another such system which is predominantly one-dimensional magnetically although the relatively small anisotropy in the resistivity (a factor of two with higher resistivity along c) indicates the charge carriers are not restricted to the c -axis.

We would like to thank the technical staff of ISIS and Chalk River Laboratories for expert assistance with the neutron scattering measurements described in this paper. This work was financially supported by NSERC and the CIAR.

References

- [1] T.E. Mason, G. Aeppli, S.M. Hayden, A.P. Ramirez, and H.A. Mook, *Physica B* **199&200** (1994) 284 and references therein.
- [2] E. Fawcett, H.L. Alberts, V. Yu. Galkin, D.R. Noakes, and J.V. Yakhmi, *Rev. Mod. Phys.* **66** (1994) 25.
- [3] W. Bao, C. Broholm, S.A. Carter, T.F. Rosenbaum, and G. Aeppli, *Phys. Rev. Lett.* **71** (1993) 766.
- [4] H.J. Walbaum, *Z. Metallknd.* **35** (1943) 218.
- [5] L.M. Corliss, J.M. Hastings, W. Kunmann, R. Thomas, J. Zhuang, R. Butera, and D. Mukamel, *Phys. Rev. B* **31** (1985) 4337.
- [6] Yu.A. Dorofeyev, A.Z. Menshikov, G.L. Budrina, and V.N. Syromyatnikov, *Phys. Met. Metall.* **63** (1987) 62.
- [7] A.Z. Menshikov, Yu.A. Dorofeyev, G.L. Budrina, and V.N. Syromyatnikov, *J. Magn. Magn. Mat.* **73** (1988) 211.
- [8] J.B. Forsyth, C.E. Jonson, and P.J. Brown, *Phil. Mag.* **10** (1964) 713.
- [9] R.P. Krentsis, A.V. Mikhel'son, and P.V. Gel'd, *Sov. Phys. Sol. Stat.* **12** (1970) 727.
- [10] R.P. Krentsis, K.I. Meizer, and P.V. Gel'd, *Sov. Phys. Sol. Stat.* **14** (1973) 2601.
- [11] V. Pluznikov, D. Feder, and E. Fawcett, *J. Magn. Magn. Mat.* **27** (1982) 343.
- [12] A.V. Mikhel'son, R.P. Krentsis, and P.V. Gel'd, *Sov. Phys. Sol. Stat.* **12** (1971) 1979.
- [13] V.V. Tarasenko, V. Pluzhnikov, and E. Fawcett, *Phys. Rev. B* **40** (1989) 471.
- [14] T.M. Holden, A.Z. Menshikov, and E. Fawcett, *J. Phys.: Condens. Matter* **8** (1996) L291–L294.
- [15] C.P. Adams, T.E. Mason, S.A.M. Mentink, and E. Fawcett, *J. Phys.: Condens. Matter*, submitted (1996).
- [16] C.P. Adams, T.E. Mason, E. Fawcett, A.Z. Menshikov, C.D. Frost, J.B. Forsyth, T.G. Perring, and T.M. Holden, in preparation (1996).